Catal Lett (2008) 126:241–246
DOI 10.1007/s10562-008-9620-4

From Electron Density Flow Towards Activation: Benzene Interacting with Cu(I) and Ag(I) Sites in ZSM-5. DFT Modeling

**P. Kozyra · J. Załucka · M. Mitoraj ·
E. Brocławik · J. Datka**

Received: 4 July 2008 / Accepted: 12 August 2008 / Published online: 9 September 2008

Abstract Cu(I) and Ag(I) sites in ZSM-5 and their interaction with adsorbed benzene are studied by DFT cluster modeling aided with NOCV analysis of charge transfer processes. The interplay between donation and back donation from the cation to the ad-molecule, reinforced by the framework environment correlates with benzene activation shown also by the red shift in calculated and measured IR frequencies. Copper sites have better activation ability due to its stronger interaction with the framework, serving as electron reservoir, and better match between d orbitals and π orbitals of benzene.

Keywords Benzene activation · DFT modeling · Cu(I) sites

1 Introduction

High activity of copper sites towards NO or alkenes, promoted by its ability to donate electrons to π antibonding orbitals of the adsorbate is well known [1–3] while the activity of silver sites is much lower. In this work copper(I) sites are compared with silver(I) to answer the question whether benzene could be activated also by the silver and how the activation is realized. Benzene was selected since its activation is relevant for catalysis as the source of phenol produced by one step oxidation of benzene over zeolite CuZSM-5 [4].

Copper sites in ZSM-5 have already been studied extensively with respect to their siting and catalytic properties by theoretical modeling with DFT cluster, embedded cluster or periodic calculations [5–9]. Our group combined IR experiment with cluster DFT cluster modeling to shed some light on charge transfer processes and the origin of donation/back-donation abilities of the sites and their influence on the activation of adsorbed molecules [10–12]. Nevertheless, clear distinction between donation and back-donation processes, straightforward for simplified, fully symmetric models, was not affordable with the use of standard population analyses for more realistic cluster models incorporating part of the framework. Accordingly, the role of the framework environment could be described merely at qualitative level as the electron reservoir.

Therefore in this paper we present the results of the new method based on Natural Orbitals for Chemical Valence [13, 14] applied to cluster models of Cu(I) and Ag(I) sites in ZSM-5. NOCV analysis focuses on describing the modification of charge density (differential density) imposed by the interaction between the fragments thought either as the ad-molecule and the site or the silicalite framework and the cation with bound adsorbate. Results presented in this work allow illustrating quantitatively the synergic effect of zeolitic framework and the cation in the activation of benzene adsorbed on copper or silver sites. At the same time the differences in catalytic properties of Cu(I) and Ag(I) are discussed. Copper sites have better activation ability than silver sites due to stronger interaction of Cu(I) with the framework, serving as electron reservoir, and better match between copper d orbitals and π orbitals of benzene.

The work was presented during the conference 'Catalysis for Society', Krakow, May 11–15, 2008.

P. Kozyra · J. Załucka · M. Mitoraj · J. Datka
Faculty of Chemistry, Jagiellonian University, ul. Ingardena 3,
30-060 Krakow, Poland

E. Brocławik (✉)
Institute of Catalysis and Surface Chemistry, Polish Academy of Sciences, ul. Niezapominajek 8, 30-239 Krakow, Poland
e-mail: broclawi@chemia.uj.edu.pl

2 Methodology

Density functional theory calculations were carried out by ADF software [15–19] for the models for the adsorption system built of M_7 clusters [20], representing zeolite environment for Cu^+, Ag^+ and Na^+ cations, and benzene molecule. M_7 cluster is a fragment of ZSM-5 framework and contains 6-membered ring made of two consolidated 5-membered rings, as shown in Fig. 1. M is for “main channel”, 7 is for 7 Si or Al atoms. To saturate peripheral bonds in the model, silicon atoms from the next coordination sphere were replaced by hydrogen atoms. Positions of these hydrogens were frozen to simulate geometrical constrains imposed by the rest of the framework. Such clusters were already successfully used by us to elucidate properties of cationic sites in zeolites in conjunction with IR experiments [21]. ADF software was selected in this work to extend the scope of the study by advanced decomposition of charge transfer processes accompanying adsorption of benzene on a cationic site, provided by NOCV analysis included in the developer version of ADF.

We have used the BP gradient potential with Becke exchange [22] and Perdew correlation [23]. Calculations were carried out in TZP basis set for transition metal cations, and DZP for the rest of atoms [24]. To save computation time inner core orbitals were frozen. Initial geometry for ADF optimization was taken from the structure optimized with Gaussian 03 software. Population analysis was done according to Hirshfeld method [25].

The interaction between the cationic sites of ZSM-5 and the benzene species have been analyzed using the Natural Orbitals for Chemical Valence [13, 14] and Ziegler–Rauk energy decpomposition scheme [26, 27].

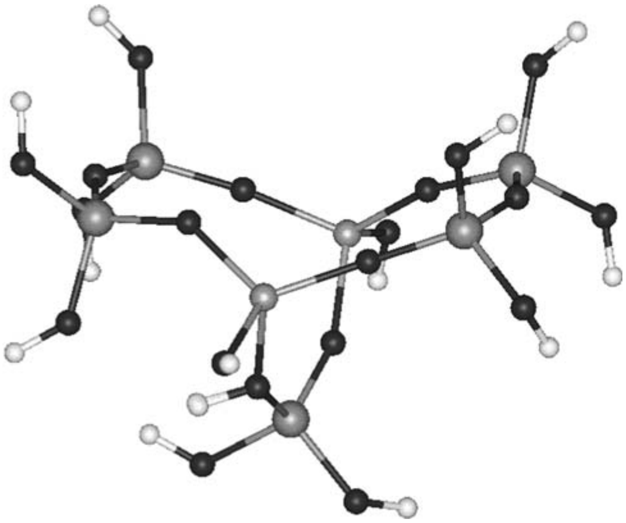

Fig. 1 Model of M_7 cluster

The Natural orbitals for Chemical Valence are defined as the eigenvectors of the chemical valence operator $\hat{V}$.

$$\hat{V}\varphi_i = v_i\varphi_i \quad i = 1, \ldots, n \text{ (number of the base function)} \tag{1}$$

The valence operator is defined as:

$$\hat{V} = \frac{1}{2}(\hat{P} - \hat{P}^0) \tag{2}$$

where P—charge and bond order matrix for a molecule, P^0—charge and bond order matrix for a promolecule—the fragments placed in the same geometry as in a parent molecule but do not interact with each other.

The very useful feature of NOCV is that they decompose the deformation density (differential density, $\Delta\rho(r)$) into diagonal contributions (Eq. 3):

$$\Delta\rho(r) = \sum_{i=1}^{n} v_i\varphi_i^2(r) \tag{3}$$

It allows to address directly the Dewar–Chatt–Duncanson model of bonding [28, 29], i.e. donation and back-donation charge transfer processes between considered molecular fragments. The eigenvectors of $\hat{V}$can be coupled in pairs of orbitals with eigenvalues of the opposite sign but the same module value:

$$\hat{V}\varphi_{-k} = -v_k\varphi_{-k} \quad \hat{V}\varphi_k = v_k\varphi_k \quad k = 1, \ldots, n/2 \tag{4}$$

The few of such couples contribute to the bond formation between fragments describing density cumulating between them, while many orbitals describing electron density of the fragments do not participate in the bond formation. Thus these contributions are given as:

$$\rho_k = |v_k|\left(|\varphi_k|^2 - |\varphi_{-k}|^2\right) \tag{5}$$

Due to the Eq. 3, the absolute eigenvalues of NOCV can be treated as a direct measure of charge flow between the chosen molecular fragments. The shape of NOCV helps to attribute σ/π and donation/back-donation character of bonding.

The Ziegler–Rauk bond energy decomposition analysis was performed for the description of the bonding between the cations and benzene ring. In the Ziegler–Rauk bond decomposition scheme the total bonding energy ΔE_{bon} between interacting fragments is divided into three components. The first component ΔE_{dist}, referred to the distortion term, represents the amount of energy required to promote the separated fragments from their equilibrium geometry to the structure they will take up in the combined molecule. The second term $\Delta E_{\mathrm{steric}}$ corresponds to the steric interaction between interacting fragments. Finally, the last term ΔE_{orb} represents the interactions between the occupied molecular orbitals on one fragment with the unoccupied molecular orbitals of the other fragment as well as mixing of occupied and virtual orbitals within the same fragment (inner-fragment polarization). Two various decomposition schemes into the subsystems were probed to study various channels of charge flow: (i) ad-molecule plus a cation with cluster environment and (ii) cation with ad-molecule plus M_7 cluster.

3 Results and Discussion

The NOCV analysis is a tool which is able to show the change in electron density imposed by the interaction between the fragments of the 'supermolecule'. The choice of the way how to divide the system into promolecules is arbitrary. Having this opportunity one can elucidate the information about the system and the interaction of its parts within variety of schemes. Benzene as one promolecule and the site as the second one is a natural separation for benzene adsorbed on the cationic site and brings information about donation and back-donation processes between the cation and the ad-molecule but is not a sufficient perspective to fully follow the role of a zeolite network. An alternative scheme for the treatment of the system is needed to complete the picture, namely with the framework M_7 cluster and Cu–C_6H_6 fragment as the two subsystems.

3.1 [C_6H_6]–[Cu^+–M_7]

Within the former perspective, with an ad-molecule and a site the two subsystems, we are able to analyze the activation of benzene by its adsorption and interaction with Cu^+ site. The main contributions to differential electron density characterized the interaction of benzene with Cu^+ site (with $|\nu| > 0.1$) are shown in the Fig. 2a–d. The most significant contribution consists of π-back donation from *d*-orbital of copper cation to π-orbitals of carbon atoms in benzene molecule (Fig. 2a). It should be noticed that in spite of the fact that the cation is positively charged, the flow from the cation to the adsorbed molecule takes the lead. Only the second significant NOCV ρ_2 contribution describes donation from benzene to Cu^+ (Fig. 2b). Also the pictures 2c and 2d represent back donations from *d*-type Cu-orbitals to benzene. Certainly, copper cation receives some electrons from benzene but the back donation estimated from NOCV analysis prevails over donation (Table 1). As stated previously, the eigenvalues for two complementary natural orbitals give the information about quantitative contribution of a respective part of differential electron density into respective charge flow. On the basis of such eigenvalues donation (V_d) and back donation (V_{bd}) contribution by NOCV have been calculated and are gathered in Table 1.

The effect of charge flows, which are represented by contributions mentioned above, should be also envisaged to some extent by population analysis. Values of Hirshfeld charges summed for benzene, the cation and M_7 cluster, respectively, before and after adsorption, are shown in the Table 1. Surprisingly, apart from the expected electron transfer from the cation to benzene, population analysis suggests that for the system with copper cation zeolite, framework gains significant share of electrons in spite of its

Table 1 Benzene interacting with bare Me^+ and Me^+M_7 sites: donation (V_d) and back donation (V_{bd}) contribution by NOCV, frequency red shift ($\Delta\nu$) and charges on interacting fragments

	Cu^+		Ag^+	
	C_6H_6/Cu^+	C_6H_6/Cu^+M_7	C_6H_6/Ag^+	C_6H_6/Ag^+M_7
V_d	0.76	0.46	0.48	0.27
V_{bd}	0.54	0.70	0.00	0.38
$V_d + V_{bd}$	1.30	1.16	0.48	0.65
$\Delta\nu_{calc}$	−27	−22	−16	−11
$\Delta\nu_{exp}$	–	−16	–	−7
$\Delta Q_{benzene}$	+0.45	+0.01	+0.34	+0.04
ΔQ_{Me^+}	−0.55	+0.05	−0.66	−0.04
ΔQ_{M7}	–	−0.06	–	0.00

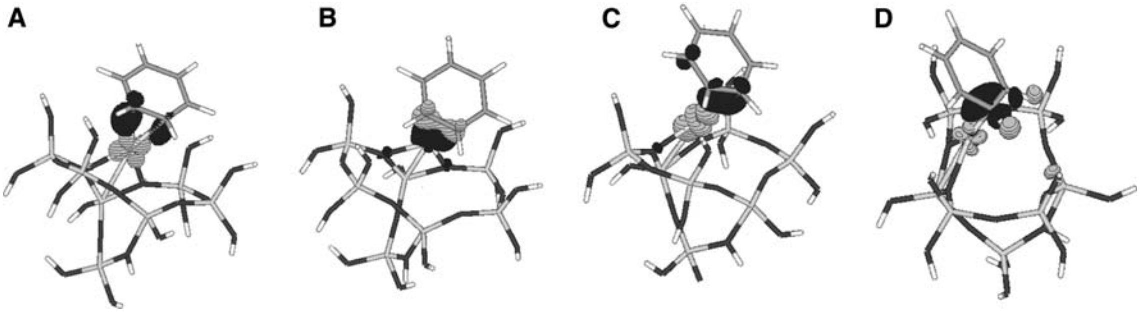

Fig. 2 Contours of the main contributions to differential deformation density for [C_6H_6]–[Cu^+M_7]. Light colour means density depletion, dark colour means density gain

Fig. 3 Contours of the main contributions to differential deformation density for [C_6H_6]–[Ag^+M_7]. Colours as in Fig. 2

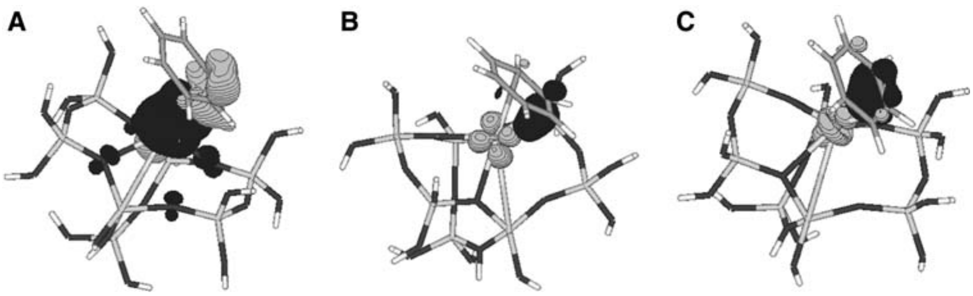

generalized anionic ligand character. This shows that charge flow processes are composed of various events executed by multiple channels. Accordingly, one could expect that the difference between donation and back donation would correlate with a charge on benzene molecule. However, donation and back-donation processes not always can be interpreted as complete electron transfers from one fragment to the other one. For example, Figs. 2a and 3b illustrate depopulating metal d orbitals but the increase of electron density is localized not only on benzene carbons but also in the bonding region between the fragments. Therefore the effective result of donation and back donation cannot be identified with the change in atomic population.

Although silver cation has the same electron configuration as copper cation, it behaves in a different way when interacting with benzene. Contrary to copper site, the most significant contribution of benzene interaction with silver site is the donation from benzene to the cation (Fig. 3a). In the case of Ag^+ π-back donation can be identified within consecutive NOCV orbitals (Fig. 3b, c) as the second and third component of differential electron density. Eventually, back donation and donation are nearly balanced while population analysis yields positive charge on benzene.

3.2 [Cu^+–C_6H_6]–[M_7]

The results presented in the previous paragraph have led to not fully consistent picture of charge flow processes between the fragments defined as the separate benzene molecule (in the geometry distorted by prospective adsorption) and [Me^+–M_7] model of the active site (also distorted by prospective interaction with the ad-molecule). In particular the electron outflow from the copper towards already negative framework could not be straightforwardly understood. This stemmed from the lack of detailed information on the charge flow between two parts of the same fragment.

Therefore we have performed NOCV analysis with alternative decomposition of adsorbed system into the fragments: sole zeolitic cluster [M_7] and the cation interacting with benzene, [Me^+–C_6H_6], in attempt to separate to some extent the two charge redistribution processes. Figures 4 and 5 show the most important NOCV contributions (with $|\nu_k| > 0.1$) for Cu^+ and Ag^+ systems, respectively. It is evident that natural orbitals with alternative fragmentation provide more information about the framework role in electron density redistribution than the former (seemingly more natural) decomposition while they barely describe density deformation imposed by intra-fragment interaction. The selected important deformation density contributions clearly do not carry the information on the donation of electrons from benzene to the cation which shows that this process takes place already in the isolated fragment. Indeed, NOCV analysis performed for benzene interacting with bare cations in stationary geometries of these systems [30] has shown that the donation from benzene π orbitals populates mainly empty s-like orbital of the cation (see Fig. 6). Obviously, NOCV orbitals yielding the share in donation effect in the composed [M_7]–[Me^+–C_6H_6] system (Fig. 2b, 3a), are distorted with respect to fully symmetric Me^+–C_6H_6 system due to different geometrical arrangement in the former case.

Fig. 4 Contours of the main contributions to differential deformation density for [C_6H_6–Cu^+]–[M_7]. Colours as in Fig. 2

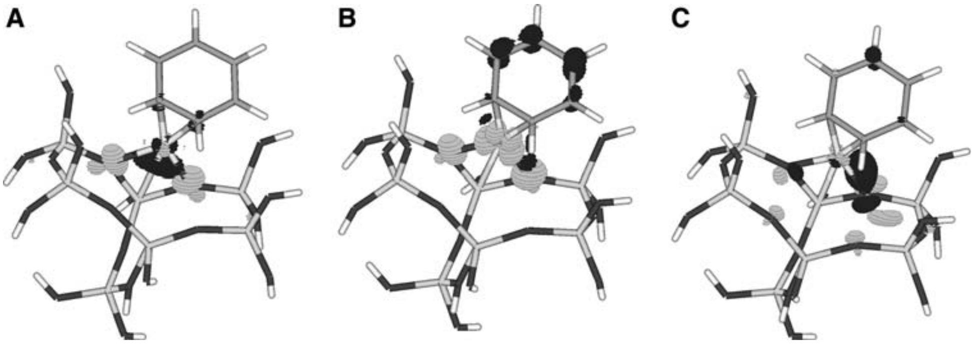

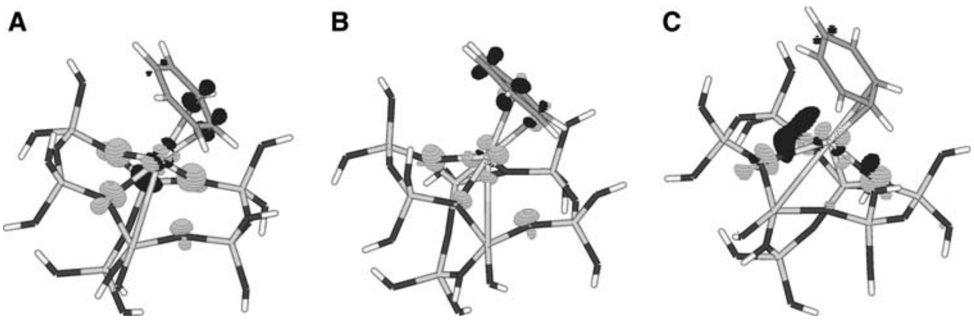

Fig. 5 Contours of the main contributions to differential deformation density for [C_6H_6–Ag^+]–[M_7]. Colours as in Fig. 2

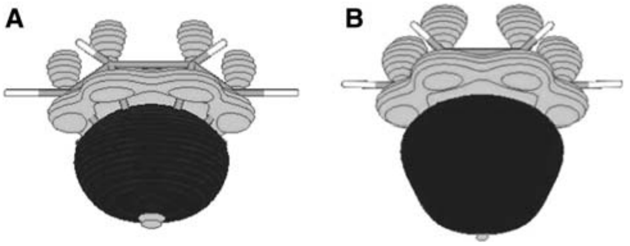

Fig. 6 Contours of differential density contribution describing donation from benzene to the cation for Cu^+–C_6H_6 (**a**), Ag^+–C_6H_6 (**b**). Colours as in Fig. 2

Table 2 Benzene adsorbed on Me^+M_7 sites: total bonding energy (E_{tot}), orbital energy (E_{orb}), steric energy (E_{steric}) for two alternative decomposition schemes into fragments

		$C_6H_6Cu^+M_7$	$C_6H_6Ag^+M_7$
C_6H_6/Me^+M_7	E_{tot}/kcal mol^{-1}	−32	−15
	E_{orb}/kcal mol^{-1}	−51	−19
	E_{steric}/kcal mol^{-1}	19	4
$C_6H_6Me^+/M_7$	E_{tot}/kcal mol^{-1}	−143	−128
	E_{orb}/kcal mol^{-1}	−61	−49
	E_{steric}/kcal mol^{-1}	−82	−79

The NOCV contributions to the deformation density in a joint, fully interacting system are shown in Figs. 4 and 5 for [C_6H_6–Cu^+]–[M_7] and [C_6H_6–Ag^+]–[M_7], respectively. They describe various charge flow processes, as well the flow between the two subsystems as the release of intra-fragment deformation density due to geometrical stresses in separated fragments with geometry distorted from the optimum. Consecutive effects are more apparently separated for Cu^+ than for Ag^+ due to stronger interaction of the former one with zeolite framework [12], nevertheless qualitative information is analogous. The deformation density contributions carry the information not only on the charge flow between two fragments but also on the intra fragment density release after lifting geometrical strain. The main contribution (Fig. 4a) illustrates the electron flow from M_7 to Cu^+ and from Cu^+ to benzene; however, the two processes employ different channels. The second NOCV contribution (Fig. 4b) describes synergic depopulation of bridging oxygens and copper d orbital; benzene carbons non-bonded to the site regain electron density to cover its loss upon geometry deformation, not intrinsic for isolated fragment. The last contour presented in Fig. 4c illustrates density flow triggered by the loosening of the bond between bridging oxygen atoms (O_b, gaining electrons) and the copper, together with internal lattice polarization.

Table 2 shows total interaction energies between the fragments and its decomposition according to two division schemes discussed above. The first scheme focuses on binding between benzene and the site whereas the second division underlines the binding between the framework and the cation with adsorbed molecules. The bonding with the framework (second scheme) is much stronger than the bonding of benzene (first scheme). Nevertheless, the main component of benzene bonding is orbital interaction is while steric contribution (containing electrostatic interaction) prevails in bonding with framework. The latter component of interaction energy with the framework is nearly the same in the case of Cu(I) and Ag(I). On the contrary, for Cu(I) the orbital part of benzene interaction with the site is much bigger than the one for Ag(I), which may be responsible for stronger activation of benzene on Cu(I) ZSM-5, clearly visible also in the red-shift of benzene IR frequencies.

4 Conclusions

The partition of the adsorbed system into separate framework and Me^+–C_6H_6 fragments adds important information on the role of the framework in the cation ↔ benzene charge flow. Therefore joint discussion of the analyses performed for both partition schemes is necessary to fully understand benzene activation mechanism on Me^+ sites in zeolites. Benzene to cation donation is already well represented in its interaction with bare Me^+; the presence of the framework reinforces the process: bridging oxygens accept part of excess electron density getting back their share from weakened O_b–Me^+ bonds. On the other hand, electron-reach basic framework donates electrons to the cation which in turn reinforces its back-donation capacity. In summary, activation ability of the cationic site must be described as the *synergic effect of zeolitic framework and the cation*. Therefore both components are very important to understand catalytic properties of the site: the cation should be apt to donate electrons into the ad-molecule (presence of filled d shell) and the lattice basic oxygens must interact with the cation serving both as the electron donor and acceptor. The cation should be partly neutralized while Pauli repulsion between its 3d orbitals and nonbonding orbitals on O atoms should increase 3d orbital energy facilitating charge transfer from the cation to the ligand [31].

Acknowledgment This study was sponsored by the Ministry of Science and Higher Education (grant No N N 204 1987 33).

References

1. Broclawik E, Datka J, Gil B, Kozyra P (2002) Top Catal 75:353
2. Datka J, Broclawik E, Kozyra P, Kukulska-Zając E, Bartula D, Szutiak M (2004) Stud Surf Sci Catal 154:2151
3. Datka J, Kozyra P, Kukulska-Zając E, Kobyzewa W (2005) Catal Today 101:117
4. Kubacka A, Wang Z, Sulikowski B, Corberan VC (2007) J Catal 250:184
5. Sierka M, Sauer J (2005) In: Yip S (ed) The handbook of materials modelling. Springer, Dordrecht, p 241
6. Berthomieu D, Delahay G (2006) Catal Rev 48:269
7. Pietrzyk P, Gil B, Sojka Z (2007) Catal Today 126:103
8. Rejmak P, Sierka M, Sauer J (2007) Phys Chem Chem Phys 9:5446
9. Benco L, Bucko T, Grybos R, Hafner J, Sobalik Z, Dedecek J (2007) J Hrusak 111:586
10. Broclawik E, Datka J, Gil B, Piskorz W, Kozyra P (2000) Top Catal 11/12:335
11. Datka J, Broclawik E, Kozyra P, Kukulska-Zajac E, Bartula D, Szutiak M (2004) Stud Sur Sci Catal 154:2151
12. Zalucka J, Kozyra P, Mitoraj M, Broclawik E, Datka J (in press) Pol J Chem
13. Michalak A, Mitoraj M, Ziegler T (2008) J Phys Chem A 112(9):1933
14. Mitoraj M, Michalak A, Organometallics (2007) Organometallics 26(26):6576
15. Te Velde G, Bickelhaupt FM, Baerends EJ, Fonseca Guerra C, Van Gisbergen SJJ, Snijders JG, Ziegler T (2001) J Comput Chem 22:931, and refs therein
16. Baerends EJ, Ellis DE, Ros P (1973) Chem Phys 2:41
17. Baerends EJ, Ros P (1973) Chem Phys 2:52
18. Te Velde G, Baerends EJ (1992) J Comput Phys 99:84
19. Fonseca CG, Visser O, Snijders JG, te Velde G, Baerends EJ (1995) In: Clementi E, Corongiu G (eds) Methods and techniques in computational chemistry, METECC-95. STEF, Cagliari, Italy, p 305
20. Nachtigallová D, Nachtigall P, Sierka M, Sauer J (1999) Phys Chem Chem Phys 1:2019
21. Kukulska-Zając E, Kozyra P, Datka J (2006) Appl Catal A 307:46
22. Becke AD (1988) Phys Rev A 38:3098
23. Perdew JP (1986) Phys Rev B 33(12):8822
24. Delley B (1990) J Chem Phys 92:508
25. Hirshfeld FL (1977) Theor Chim Acta B 44:129
26. Ziegler T, Rauk A (1978) Theor Chim Acta 46:1
27. Ziegler T, Rauk A (1979) Inorg Chem 18:1755
28. Dewar MJS (1951) Bull Soc Chim 18:C71
29. Chatt J, Duncanson JA (1953) J Chem Soc 3:2939
30. material in preparation for separate publication
31. Davidová M, Nachtigallová D, Nachtigall P (2004) J Phys Chem B 108:13674